An Algorithm for the Visualization of a Terrain with Objects

FLÁVIO SZENBERG[1], MARCELO GATTASS[1], PAULO CEZAR PINTO CARVALHO[1,2]

[1]TeCGraf - Grupo de Tecnologia em Computação Gráfica, PUC-Rio
Rua Marquês de São Vicente, 255, 22453-900, Rio de Janeiro, RJ, Brasil
{szenberg, gattass, pcezar}@tecgraf.puc-rio.br

[2]IMPA - Instituto de Matemática Pura e Aplicada
Estrada Dona Castorina, 110, 22460-320, Rio de Janeiro, RJ, Brasil
pcezar@visgraf.impa.br

Abstract. This article describes a method for object and terrain visualization by means of the combination of two algorithms, one for terrain data and one for objects. Our purpose is to generate, efficiently and rapidly, aerial images of terrain with objects such as houses, vehicles, and transmission lines, thus allowing a simulated flight. For the objects, described by lines and polygons, the Z-Buffer algorithm is used; for the terrain, described by height maps, an optimized Ray-Casting Algorithm, called Floating Horizon Algorithm, is used.

Keywords: Terrain Visualization, GIS, Voxel-Based Modeling, Ray Casting, Interactive Visualization.

1 Introduction

This article describes a method for object and terrain visualization by means of two algorithms, one specific for terrain data and the other for objects described by polygons and lines. Our purpose is to generate, efficiently and rapidly, aerial images of terrain with objects such as houses, vehicles, and transmission lines, thus allowing a simulated flight.

In this kind of application, we are primarily concerned with algorithm performance, in order to make interactive navigation possible. An obstacle to be tackled is that the detailed geometry and texture representation of terrain surfaces demands a large amount of memory. Moreover, even though the portion of the terrain involved in a scene represents, generally, a small part of this information, its visualization using a generic graphical system may not yield the necessary efficiency. Such issues have motivated researches both in techniques for compact vector or raster terrain representations, and in optimized visualization algorithms ([LaMothe95] and [Freese+95]).

In the present work we consider the situation in which the scene contains, apart from the terrain, vector objects represented by polygons and lines. These objects can be visualized very efficiently by the standard graphical systems available in modern workstations and PCs, such as OpenGL.

We have compared the results obtained with two approaches for scene visualization containing terrain and vector objects. The first one consists in using the OpenGL graphical system for visualizing both terrain and objects. The second approach consists in using an optimized algorithm for visualizing the terrain; the image and the depth information obtained are then transferred to OpenGL, to be integrated in the scene containing the objects. Comparative results of both approaches are presented.

2 Problem Description

From the conceptual point of view, a terrain may be seen as a geographical field [Camara+96] characterized by the heights associated to points of a reference surface. In the present work, we consider only terrains having moderate dimensions, for which the reference surface can be taken as a plane.

The computer representation of a terrain surface involves, necessarily, some form of discretization, either by means of a grid (usually regular) or of a Triangular Irregular Net (TIN). In this work, terrain surfaces are represented by regular grids described by two two-dimensional matrices of equal dimensions, one determining the height at each point (height map) and the other determining the texture (color map). Examples of these maps are illustrated in Figure 1. These images were generated by the VistaPro program [VistaPro] and altered to include the highway. The images generated by VistaPro have an implicit illumination, which contributes to increase the degree of realism without degrading the visualization algorithm with expensive illumination models.

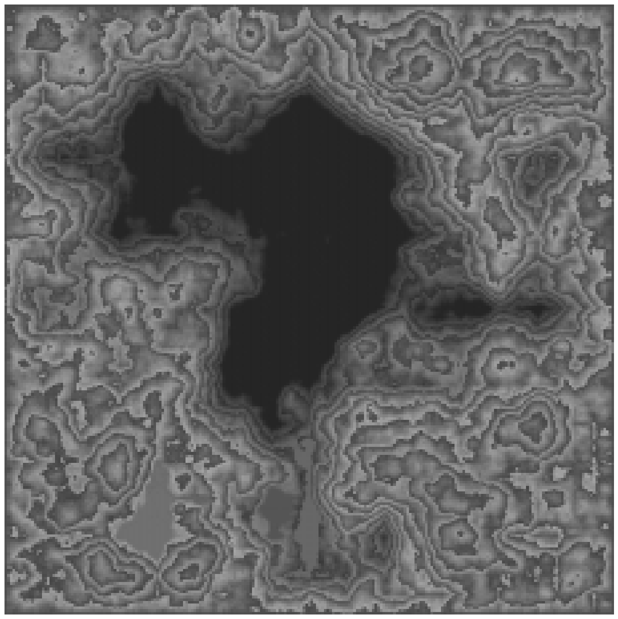
(a) Height Map

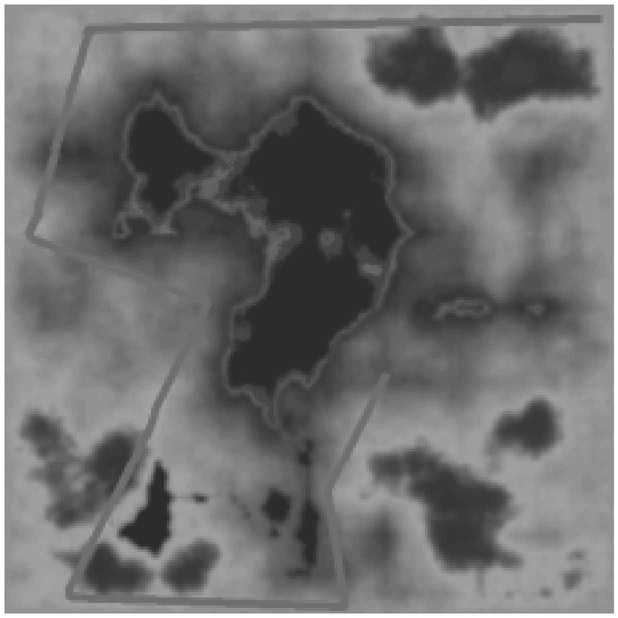
(b) Color Map

Figure 1 - Terrain Maps

The form of representation described above immediately provides a geometric model for a terrain, which can be considered as a set of rectangular blocks aligned by the axes, with width and length equal to the width of each element of the regular grid and height given by the corresponding value on the height map. If we associate to each face of each of these blocks the color provided by the corresponding element on the texture map, we will have a vector model of the terrain, which can thus be visualized by means of a generic system such as OpenGL. The advantage of this approach is the immediate integration of vectorial objects to the terrain, since the same description is used for the terrain and for the objects. The great disadvantage is the large number of faces to be visualized, which can obstruct the interactive visualization. Such issues are discussed in Section 3.

An alternative consists in looking at the terrain through the volumetric perspective. In this case, we consider that the blocks describe space occupation by the terrain. Due to this interpretation, in the games literature ([Freese+95] and [LaMothe95]) it is common to call each of these blocks a *voxel* (volume pixel). As will be seen in Section 4, image-based volume visualization algorithms can be optimized for terrain visualization, fulfilling the interactive visualization requirement. The use of such algorithms, however, is made difficult by the presence of vector objects to be added in scene. One solution is to obtain a volumetric representation of the objects to be put in scene, as is proposed in [tvcg+96]. Such a solution, nevertheless, besides involving considerable pre-processing effort, does not work for arbitrary objects: the terrain structure must be preserved after the objects are placed. In other words, each object must lie on the terrain and each vertical straight line with points common to the terrain must intersect it in alive segment having an end on the terrain.

Other suggestions for simultaneous visualization of terrain and objects are presented in [Cohen+94], [Graf+94], [Paglieroni+94] and [GuGaCa97]. [Sawyer97] describes a use for interactive visualization of terrain with objects in games such as flight simulators.

In Section 5 we will investigate another alternative for incorporating vector objects to terrain, in which terrain and objects are processed separately, making use of efficient algorithms for each kind of data. The resulting images of each process are then combined into only one image, taking into account depth information extracted from each algorithm.

3 Terrain Vector Rendering

Terrain modeled as a set of blocks, as described in the previous section, can be visually represented by:

(a) center points on top faces; (b) top faces; (c) frontal faces; (d) vertical straight line segments; and (e) the blocks themselves (constituted by 6 faces). Visualization speed and quality of the generated image quality must be considered when choosing one of those representations.

Figure 2 illustrates the images obtained by the Z-Buffer algorithm for each of the above representations.

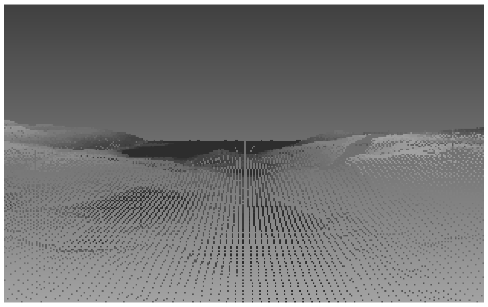
(a) Points on top faces

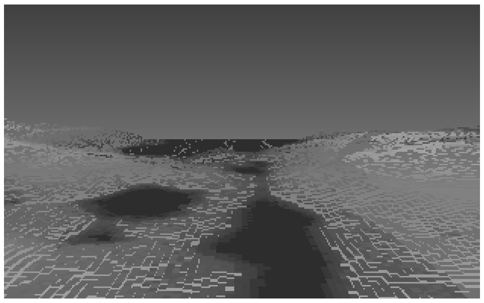
(b) Top faces

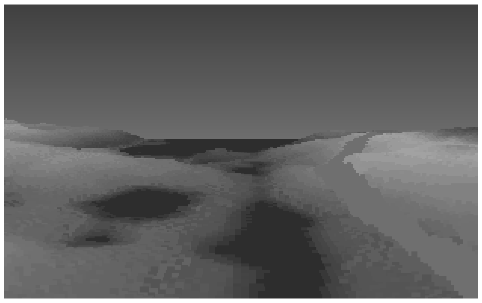
(c) Frontal faces

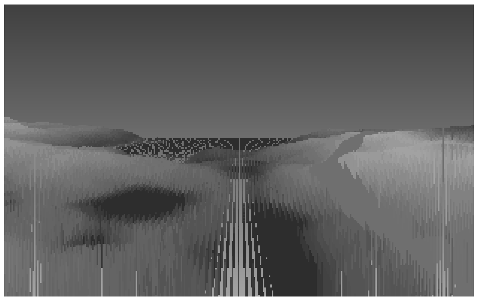
(d) Straight line segments

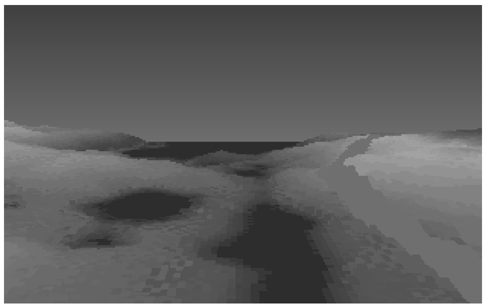
(e) Blocks

Figure 2 - Terrain Visualization with Z-Buffer.

All times shown in Table 2 are too large to support interactive visualization. To reach interactive time, of 5 frames per second, they must be reduced by a factor greater than 10. Thus, the vector representations of the terrain presented above yield unacceptable performance with the computers largely available today.

4 Efficient Terrain Algorithms

Another classical alternative for terrain rendering is the Ray Casting Algorithm. This algorithm cast rays from the observer's eye to each position in the projection plane that corresponds to a pixel in the screen. The color of this pixel is obtained from the Color Map in the intersection position between the ray and the terrain surface. If no special consideration is given, however, the efficiency of this algorithm is bound to be very low, since the number of intersections to be computed is very high. Consider, for instance, a screen with 320x200 pixels and a terrain with a 512x512 grid. The number of intersections in this case is over 16 billions per frame. It is dear that this strategy does not achieve interactive time. Therefore, an optimized version is necessary.

We will assume that the observer's head is vertical and the projection plane is perpendicular to the *xy* terrain grid, as shown in Figure 3. In this position the rays casted from the observer's eye to each column of pixels in the view plane are contained in a plane which is also perpendicular to the *xy* plane. This plane, indicated in Figure 3 as *sampling plane*, largely simplifies the visualization problem. Only the terrain voxels which are intersected by this plane can influence the color of the view plane column's pixels. Furthermore, if the voxels are sampled at uniform spaces along the intersection, the projection is reduced to a simple 2D problem, as illustrated in Figure 4.

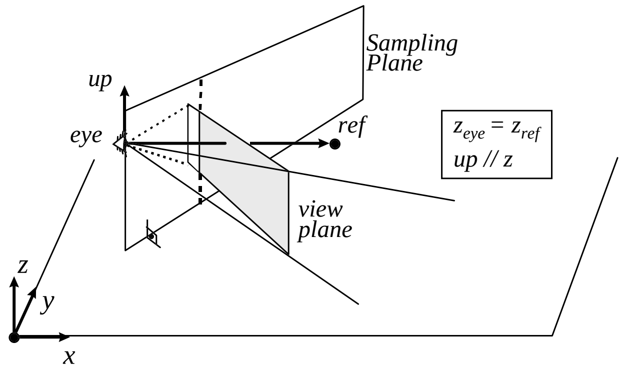

Figure 3 - Camera's special position.

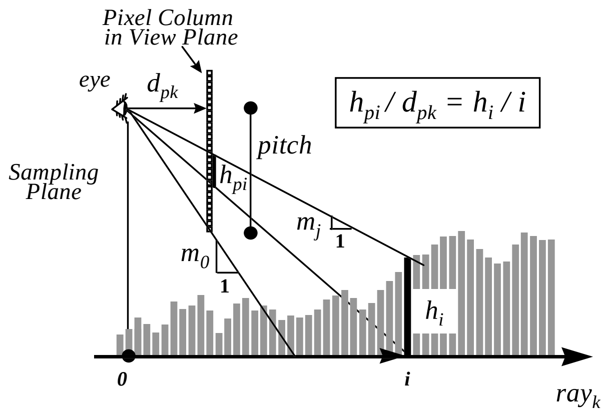

Figure 4 - Simple conic projection.

Algorithms that explore the terrain's particular model can be easily found in game programming literature ([LaMothe95] and [Freese+95]). These algorithms treat each screen column separately and paint, for each column, the pixels from the bottom of the screen upward, following the idea of a floating horizon. The Floating Horizon Algorithm starts by casting the first horizon, shown as m_0 in Figure 4. In order to determine the color of the bottom screen pixel, the algorithm tests the height of each column starting at the observer's foot, marked as ***O*** in Figure 4, and moving forward in the ray_k direction. The first column which rises above the horizon causes the pixel to be painted and the horizon to move upward. The algorithm make use of the fact that terrain voxels which are further away in the ray_k direction can not obscure the pixels already painted.

An implementation of the Floating Horizon Algorithm for a pixel column is illustrated in Algorithm 1.

Note that, as we move from one position *i* to the next, the horizon height decreases by the value of the current horizon slope, m_j, as shown in line 6 of Algorithm 1.

```
CastRay(col, pitch, dx, dy) {
1     x = eye_x; y = eye_y; z = eye_z;
2     j = 0   bottom pixel in the column
3     m = pitch/dpk;   first horizon
4     i = 0;   voxel at foot position
5     while (i < f) {   f is far
        Step in ray_k direction
6       y += dy; x += dx; z -= m;
        Gets h from the height map
7       h = HeightMap(x,y);
8       if (h > z) {   height above horiz.
9         c = ColorMap(x,y);
10        do {
            paint the pixel
11          ColorBuffer[col,j] = c;
            move one pixel up
12          j += 1;
            update horizon coef.
13          m -= 1/dpk;
            correct horizon height
14          z += i/dpk;
15          } while (h > z);
16      }   end if
17      i += 1;   next voxel
18    }   end while
19  }   end CastRay
```

Algorithm 1 - Terrain floating horizon.

Figure 4 also shows that the slope of the first horizon is given by:

$$m_0 = pitch / d_{pk} \qquad (1)$$

and the change in the slope, as we move up from pixel *j* to *(j+1)* at voxel *i*, can be given by:

$$m_{j+1} = (pitch - (j+1)) / d_{pk} = m_j - 1/ d_{pk} \qquad (2)$$

Lines 3 and 12 of Algorithm 1 show, respectively, the initialization and the update of the horizon slope.

The change in the horizon height, z¸ at voxel position *i*, can be computed by setting h_{pi} equal to 1 in the equation shown in Figure 4, yielding the equation shown in Line 13 of Algorithm 1. The division in this line of the algorithm can be easily avoided by computing this change incrementally. For the sake of clarity we present the algorithm without implementation optimizations, which are left to the reader.

To increase the speed of the Floating Horizon Algorithm applied to terrain maps, [Freese+95] and [LaMothe95] suggest two approximations: [a] all pixel columns are at same distance from the eye, i.e., d_{pk}=d_p;

and [b] the angle between two consecutive sampling planes is constant.

Frederick *et all* [Frederick+96] have shown that these approximations distort the resulting images. To combine two different algorithms, one must not accept any distortion in one of them which is not present in the other. If this is not so, a building, for example, would be moved in the terrain as the position where it is located gets distorted. For this reason, no approximation in the conic projection is allowed for the purpose of this paper.

5 Image Composition

The strategy proposed in this paper to combine the Z-Buffer with the Floating Horizon Algorithm is illustrated in Figure 5.

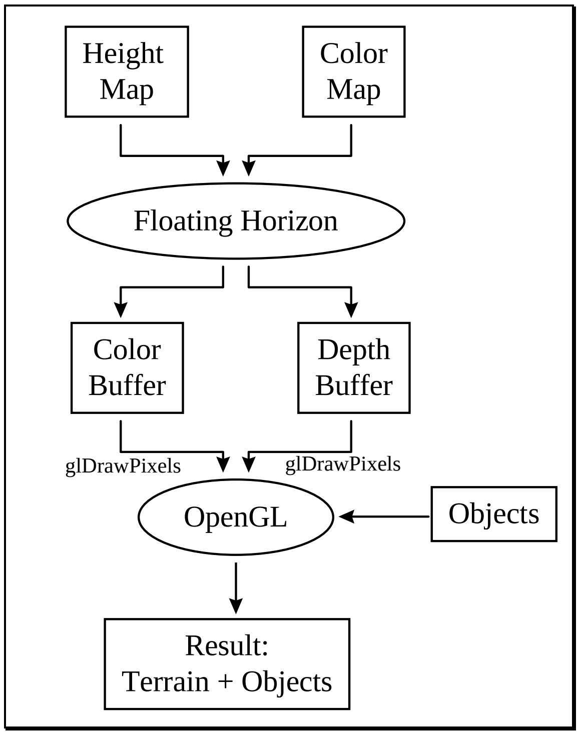

Figure 5 - Strategy to combine both algorithms.

5.1 Camera Model

The projection in OpenGL is defined in a camera model defined by the following parameters: ***eye***, ***ref***, ***up***, *left*, *right*, *bottom*, *top*, *near*, and *far*.

The conic projection used in the Floating Horizon Algorithm is defined by: [a] the observer's position which is equivalent to the ***eye***; [b] a view angle which can be easily used to define the ***ref*** point; [c] a distance to the projection point $d_p = 1$, which can be assumed to be *near*; [d] a number of terrain slices (steps) in the ray_k direction which can be assumed to be equal to *far*; and [e] a camera angle and a *pitch* which can be used to compute the OpenGL window as shown in Figure 6.

Note in figure 6 that the factor *h/w* is required to maintain the aspect ratio between the window in the projection plane and the window where the image is to be drawn.

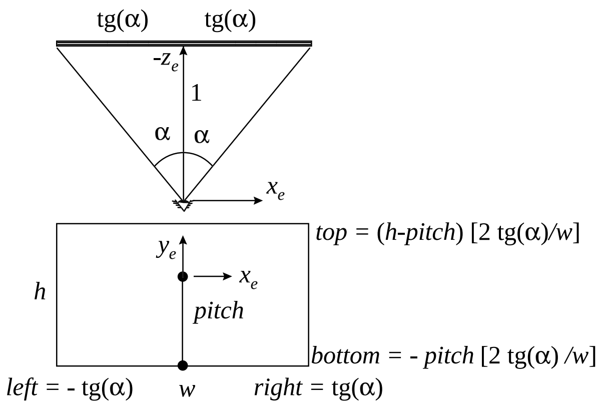

Figure 6 - Parameters for the OpenGL camera.

5.2 Depth Computation

To combine images generated by the Floating Horizon Algorithm with the Z-Buffer primitives, the depth value of each pixel in the terrain image is needed. As shown below, this depth is a function of the distance from the corresponding point in the terrain to the projection plane. This suggests a slight modification in Algorithm 1. In the version described in section 4, one steps along the terrain in unit steps; thus, the points where the terrain is sampled belong to the circles shown in Figure 7. For the purposes of depth computation, it is more convenient that we sample the terrain in slices which are parallel to the screen, represented by the dashed lines in Figure 7.

This also makes the processing of each pixel column more efficient. In the original version, each column screen *k* has its own set of slopes and height variations, which are inversely proportional to the distance d_{pk} between the eye and that column. Therefore, these coefficients differ from the ones corresponding to the central column by the factor $\cos\theta_k$. However, if the terrain is sampled according to the dashed lines, horizontal steps are corrected by the factor $1/\cos\theta_k$, causing the height variations to be the same as the ones in the central column. Therefore, slope and height updating becomes the same for all columns, provided that the unit vector (*dx*, *dy*) is scaled by the factor $1/\cos\theta_k$ for each column *k*. Note that this produces the same gain in efficiency as the simplifications proposed by [LaMothe95] and [Freese+95] without the undesired distortions.

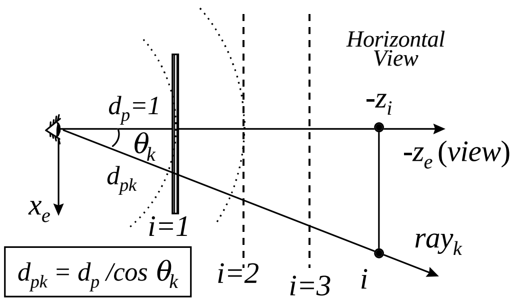

Figure 7 - Distances in ray_k direction.

Even with the above simplification, depth computation for all slices *i* is still expensive, due to the non-linear nature of the conic projection. This relation can be obtained by the homogeneous matrix, *P*, given by equation (3). This matrix is used by OpenGL ([Neider+93] and [Martha+94]) to transform between the eye and the screen coordinate systems.

$$[P] = \begin{bmatrix} \frac{2n}{r-l} & 0 & \frac{r+l}{r-l} & 0 \\ 0 & \frac{2n}{t-b} & \frac{t+b}{t-b} & 0 \\ 0 & 0 & -\frac{f+n}{f-n} & -\frac{2fn}{f-n} \\ 0 & 0 & -1 & 0 \end{bmatrix} \tag{3}$$

where *l, r, t, b, n, f* stand for *left, right, top, bottom, near* and *far*, respectively.

Thus the screen coordinate, z_s, can be computed from the eye coordinate, z_e, by:

$$z_s = \frac{(f+n) + \frac{2fn}{z_e}}{f-n} \tag{4}$$

OpenGL also provides a function called `glDepthRange`, which specifies a linear mapping between the depth range [-1,1] and a chosen depth range. The default values for this new range are 0.0 for the *near* and 1.0 for the *far* distance. With these values, Equation (4) must be modified by:

$$z_s' = \frac{z_s + 1}{2} \tag{5}$$

With the above modifications, Algorithm 1 steps through the terrain model in slices parallel to the projection plane, as shown in Figure 7. The coordinate z_e as a function of the slice *i* is then given by:

$$z_e = -i \tag{6}$$

Replacing equations (6) in (4) and (4) in (5) we can have the depth value for each slice *i* given by

$$depth = \frac{f - \frac{f \times n}{i}}{f-n} \tag{7}$$

It is important to note that this relation is invariant with the pixel column, the observer's position, and the view direction. That is, we can pre-compute all depths and store them in a vector of dimension *far*. It is important to note, however, that all these simplifications are only valid in the case where the view direction is horizontal, as shown in Figure 3.

6 Implementation

The terrain rendering implementation in the strategy proposed in Figure 5 follows Algorithm 1 with the following changes: [a] variable d_{pk} is assumed to be constant and equal to 1; [b] the norm of increment (*dx, dy*) is not 1, but $1/\cos\theta_k$, as explained in section 5.2; and [c] every time a voxel is painted, its depth is stored in the depth buffer. This is done by including the following line code just after line 11 in Algorithm 1:

```
11A DepthBuffer[col,j] = Depth[i];
```

We are assuming here that the depth vector has already been pre-computed in the beginning of the program by means of the procedure shown in Algorithm 2.

```
DepthVector(n,f) {
  for (i=0; i<=(f-n); i++)
      Depth[i]=(f-(f*n)/i)/(f-n);
}
```

Algorithm 2 - Depth vector computation.

7 Tests

To test the ideas presented here, the terrain model illustrated in Figure 1 was rendered; the resulting image is shown in Figure 8.

When the objects shown in Figure 9 are inserted in the terrain model according to the plan shown in Figure 10, the result are images such as the one shown in Figure 11.

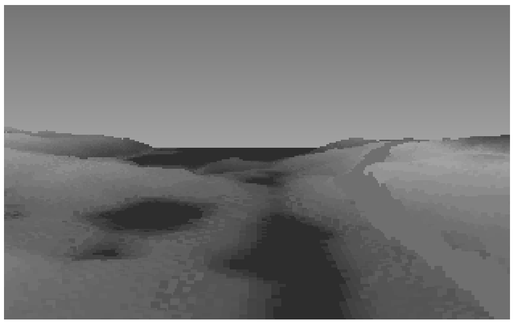
Figure 8 - Image generated by Floating Horizon.

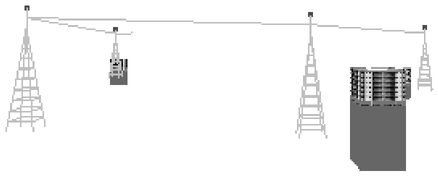
Figure 9 - Objects to be added to the terrain

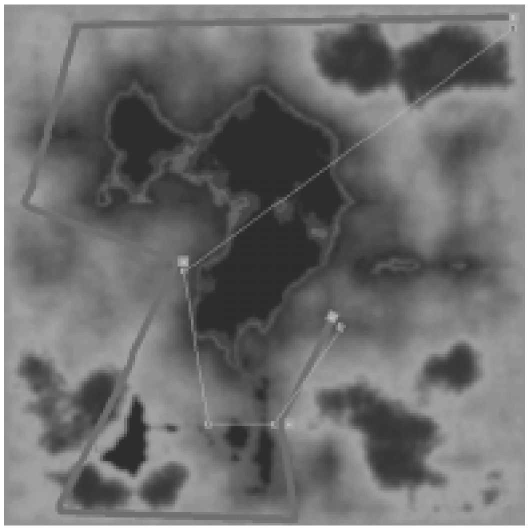
Figure 10 - Plan view of terrain and objects.

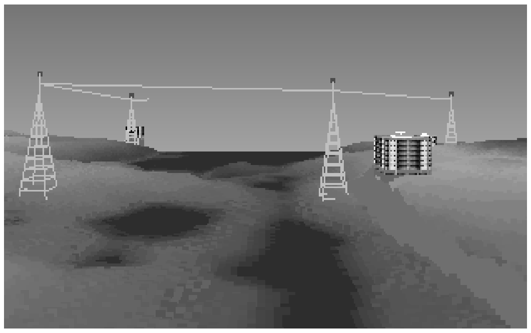
Figure 11 - Image with terrain and objects.

To evaluate the efficiency of the proposed strategy we measured the performance of the algorithm in two different computers: a PC Pentium 166 MHz, and a Silicon Indigo 2. The average time to generate a frame in two animated sequences is shown in Table 1. The first sequence renders the terrain with the objects (Figure 11) and the second renders the terrain without the objects (Figure 8). Average times were computed using 10 frames.

Note, in Table 1, that the time spent in depth computation in the Floating Horizon Algorithm is very small. The largest time is spent transferring the buffers to OpenGL. To load the color buffer we spent as much time as we did with the terrain rendering. To load the depth buffer we had to spend twice as much time as Floating Horizon did. The efficiency of the function responsible by these transfers, `glDrawPixels`, has been object of many discussions in the news group `news:comp.graphics.api.opengl`. It is conceivable that better results could be obtained with a more efficient version of this procedure.

8 Conclusions

The method proposed to compute depth information in the Floating Horizon Algorithm is very efficient and does not impact its performance.

Even with the low performance of the function `glDrawPixels`, the results obtained with the proposed strategy are far better than by making use of Z-Buffer to render the terrain. This fact reinforces the need for a specific algorithm to approach this class of problems.

Although the *aliasing* problem was not severe in the examples presented here, the authors believe that it may became a serious concern if real aerial photos were used.

9 Acknowledgments

This work was developed in TeCGraf/PUC-Rio and was partially funded by CAPES and CNPq, by means of fellowships, and the PROTEM/CC-GEOTEC project. TeCGraf is a Laboratory mainly funded by PETROBRAS. The authors want to thank Professors Luiz Fernando Martha (PUC-Rio) and Luiz Carlos Guedes (UFF) for their valuable suggestions.

	Terrain with objects				Terrain without objects			
	PC		SGI		PC		SGI	
Steps in the Algorithm	**t(s)**	**t(%)**	**t(s)**	**t(%)**	**t(s)**	**t(%)**	**t(s)**	**t(%)**
Floating Horizon	0.05	23	0.18	51	0.04	50	0.13	76
Z-Buffer load	0.11	50	0.11	31	-	-	-	-
Color Buffer load	0.04	18	0.04	12	0.04	50	0.04	24
Objects	0.02	9	0.02	6	-	-	-	-
Total Time	0.22	100	0.35	100	0.08	100	0.17	100
Frames/sec.	4.6		3.0		14.1		5.9	

Table 1 - Time in seconds for each step of the proposed strategy.

	Terrain with objects		Terrain without objects	
Terrain represented by	**PC**	**SGI**	**PC**	**SGI**
(a) Points on top faces	0.62	0.83	0.63	0.83
(b) Top faces	0.28	0.50	0.29	0.50
(c) Frontal faces	0.24	0.48	0.24	0.48
(d) Straight line segments	0.43	0.46	0.44	0.47
(e) Blocks	0.07	0.17	0.07	0.17

Table 2 - Frames per seconds for Z-Buffer algorithm.

10 Availability

A version of the program used in this paper for Windows95/NT and the sample files shown in Figure 1 are available in `http://www.tecgraf.puc-rio.br/~szenberg/artigo_sib97/program.zip`. With this program the user can fly over the terrain using keyboard arrows.

Bibliography

[LaMothe95] A. La Mothe, *Black Art of 3D Game Programming*, Waite Group Press, 1995.

[Freese+95] P. Freese, *More Tricks of the Game Programming Gurus*, SAMS Publishing, 1995.

[Camara+96] G. Câmara et al., *Anatomia de Sistemas de Informações Geográfica*, 10ª Escola de Computação, 1996.

[Frederick+96] P. Frederick et al., *Visualização Interativa Tridimensional de Modelos de Terreno com Textura*, Anais do IX SIBGRAPI, pp. 341-342, 1996.

[Martha+94] L. F. Martha et al., *Um Resumo das Transformações Geométricas para Visualização em 3D*, Caderno de Comunicações do VII SIBGRAPI, pp. 9-12, 1994.

[Graf+94] K. Ch. Graf et al., *Perspective Terrain Visualization - A Fusion of Remote Sensing, GIS, and Computer Graphics*, Comput. & Graphics, Vol. 18, No. 6, pp. 795-802, 1994.

[tvcg+96] D. Cohen-Or et al., *A Real-Time Photo-Realistic Visual Flytrough*, `ftp://ftp.math.tau.ac.il/pub/daniel/tiltan.ps.gz`.

[Cohen+94] D. Cohen et al., *Photorealistic Terrain Imaging and Flight Simulation*, IEEE Computer Graphics and Applications, Vol. 14, No. 2, pp. 10-12, March, 1994.

[Paglieroni+94] D. Paglieroni et al., *Height Distributional Distance Transform Methods for Height Field Ray Tracing*, ACM Transactions on Graphics, Vol. 13, No. 4, pp. 376-399, October, 1994.

[Neider+93] J. Neider et al., *OpenGL Programming Guide: the Official Guide Learnning OpenGL, release 1*, Addison-Wesley Publishing Company, 1993.

[VistaPro] VistaPro, `http://www.callamer.com/vrli/vp.html`.

[Sawyer97] B. Sawyer, *Skimming the Voxel Surface with NovaLogic's Commanche 3*, Game Developer, pp. 62-70, April-May 1997.

[GuGaCa97] L. Guedes et al., *Real Time Rendering of Photo-Texture Terrain Height Fields*, X SIBGRAPI.